Purely Salt-Responsive Micelle Formation and Inversion Based on a Novel Schizophrenic Sulfobetaine Block Copolymer: Structure and Kinetics of Micellization

ARTICLE *in* LANGMUIR · NOVEMBER 2007

Impact Factor: 4.46 · DOI: 10.1021/la702029a · Source: PubMed

5 AUTHORS, INCLUDING:

Xuejuan Wan
Shenzhen University
19 PUBLICATIONS **416** CITATIONS
SEE PROFILE

Xiaofeng Wang
University of Science and Technology of China
24 PUBLICATIONS **425** CITATIONS
SEE PROFILE

Purely Salt-Responsive Micelle Formation and Inversion Based on a Novel Schizophrenic Sulfobetaine Block Copolymer: Structure and Kinetics of Micellization

Di Wang, Tao Wu, Xuejuan Wan, Xiaofeng Wang, and Shiyong Liu*

Department of Polymer Science and Engineering, Joint Laboratory of Polymer Thin Films and Solution, Hefei National Laboratory for Physical Sciences at the Microscale, University of Science and Technology of China, Hefei, Anhui 230026, China

Received July 7, 2007. In Final Form: August 25, 2007

A novel sulfobetaine block copolymer, poly(*N*-(morpholino)ethyl methacrylate)-*b*-poly(4-(2-sulfoethyl)-1-(4-vinylbenzyl)pyridinium betaine) (PMEMA-*b*-PSVBP), was synthesized via reversible addition-fragmentation chain transfer polymerization. In aqueous solution, PMEMA homopolymer becomes insoluble in the presence of Na_2SO_4 (>0.6 M), whereas PSVBP homopolymer molecularly dissolves in the presence of NaBr (>0.2 M). Thus, PMEMA-*b*-PSVBP diblock copolymer exhibits purely salt-responsive "schizophrenic" micellization behavior in aqueous solution, forming two types of micelles with invertible structures, that is, PMEMA-core and PSVBP-core micelles, depending on the concentrations and types of added salts (Scheme 1). The equilibrium structures of these two types of micelles were characterized via a combination of ^{1}H NMR and laser light scattering (LLS). We further investigated the kinetics of salt-induced formation/dissociation of PMEMA-core and PSVBP-core micelles and the structural inversion between them employing the stopped-flow light scattering technique. In the presence of 0.5 M NaBr, the addition of Na_2SO_4 (>0.6 M) induces the formation of PMEMA-core micelles stabilized with well-solvated PSVBP coronas. Dilution-induced dissociation of PMEMA-core micelles into unimers occurs within the dead time of the stopped-flow apparatus (∼2−3 ms) when the final Na_2SO_4 concentration drops below 0.3 M, while salt-induced breakup of PSVBP-core micelles is considerably slower. The structural inversion from PMEMA-core to PSVBP-core micelles proceeds first with the dissociation of PMEMA-core micelles into unimers, followed by the formation of PSVBP-core micelles. On the other hand, structural inversion from PSVBP-core to PMEMA-core micelles exhibits different kinetic sequences. Immediately after the salt jump, PMEMA corona chains are rendered insoluble, and unstable PSVBP-core micelles undergo intermicellar fusion; this is accompanied and/or followed by the solvation of PSVBP cores and structural inversion into colloidally stable PMEMA-core micelles.

Introduction

In the past decade, increasing attention has been paid to double hydrophilic block copolymers (DHBCs).[1,2] Subjected to physical or chemical transformations, one of the blocks of DHBCs can be selectively rendered water-insoluble, while the other block still remains well-solvated to stabilize the formed colloidal aggregates. Moreover, certain DHBCs can form two or more types of aggregates with inverted structures upon judicious adjustment of external conditions, such as solution pH, temperature, and ionic strength. Since 1998, numerous examples of DHBCs exhibiting the so-called "schizophrenic" micellization behavior have been reported.[3−15] In most cases, the formation/breakup and structural inversion of DHBC micelles were induced by a combination of several external stimuli.[16−20] In some cases, manipulation of the "schizophrenic" micellization behavior of DHBCs via a single external stimulus will considerably simplify the procedure and is highly desirable.

Previous studies demonstrated that the formation and inversion of certain DHBC micelles can be realized by solely adjusting the solution pH.[21,22] Recently, Laschewsky et al. reported the first example of a purely thermoresponsive "schizophrenic" DHBC, which contained two component blocks exhibiting lower critical solution temperature (LCST) and upper critical solution temperature (UCST) phase transitions, respectively.[23,24] Following

* To whom correspondence should be addressed. E-mail: sliu@ustc.edu.cn.

(1) Colfen, H. *Macromol. Rapid Commun.* **2001**, *22*, 219−252.
(2) Minko, S. *Responsive Polymer Materials: Design and Applications*; Blackwell Publishing: Ames, IA, 2006.
(3) Luzinov, I.; Minko, S.; Tsukruk, V. V. *Prog. Polym. Sci.* **2004**, *29*, 635−698.
(4) Butun, V.; Liu, S.; Weaver, J. V. M.; Bories-Azeau, X.; Cai, Y.; Armes, S. P. *React. Funct. Polym.* **2006**, *66*, 157−165.
(5) Li, Y. T.; Armes, S. P.; Jin, X. P.; Zhu, S. P. *Macromolecules* **2003**, *36*, 8268−8275.
(6) Pispas, S. *J. Polym. Sci., Part A: Polym. Chem.* **2006**, *44*, 606−613.
(7) Bo, Q.; Zhao, Y. *J. Polym. Sci., Part A: Polym. Chem.* **2006**, *44*, 1734−1744.
(8) Vamvakaki, M.; Palioura, D.; Spyros, A.; Armes, S. P.; Anastasiadis, S. H. *Macromolecules* **2006**, *39*, 5106−5112.
(9) Zhang, W. Q.; Shi, L. Q.; Ma, R. J.; An, Y. L.; Xu, Y. L.; Wu, K. *Macromolecules* **2005**, *38*, 8850−8852.
(10) Vandermeulen, G. W. M.; Tziatzios, C.; Duncan, R.; Klok, H. A. *Macromolecules* **2005**, *38*, 761−769.
(11) Rodriguez-Hernandez, J.; Lecommandoux, S. *J. Am. Chem. Soc.* **2005**, *127*, 2026−2027.
(12) Alarcon, C. D. H.; Pennadam, S.; Alexander, C. *Chem. Soc. Rev.* **2005**, *34*, 276−285.
(13) Mountrichas, G.; Pispas, S. *Macromolecules* **2006**, *39*, 4767−4774.
(14) Andre, X.; Zhang, M. F.; Muller, A. H. E. *Macromol. Rapid Commun.* **2005**, *26*, 558−563.
(15) Ma, Y. H.; Tang, Y. Q.; Billingham, N. C.; Armes, S. P.; Lewis, A. L.; Lloyd, A. W.; Salvage, J. P. *Macromolecules* **2003**, *36*, 3475−3484.
(16) Butun, V.; Armes, S. P.; Billingham, N. C.; Tuzar, Z.; Rankin, A.; Eastoe, J.; Heenan, R. K. *Macromolecules* **2001**, *34*, 1503−1511.
(17) Butun, V.; Billingham, N. C.; Armes, S. P. *J. Am. Chem. Soc.* **1998**, *120*, 11818−11819.
(18) Gil, E. S.; Hudson, S. A. *Prog. Polym. Sci.* **2004**, *29*, 1173−1222.
(19) Liu, S. Y.; Armes, S. P. *Langmuir* **2003**, *19*, 4432−4438.
(20) Liu, S. Y.; Billingham, N. C.; Armes, S. P. *Angew. Chem., Int. Ed.* **2001**, *40*, 2328−2331.
(21) Dai, S.; Ravi, P.; Tam, K. C.; Mao, B. W.; Gang, L. H. *Langmuir* **2003**, *19*, 5175−5177.
(22) Liu, S. Y.; Armes, S. P. *Angew. Chem., Int. Ed.* **2002**, *41*, 1413−1416.
(23) Virtanen, J.; Arotcarena, M.; Heise, B.; Ishaya, S.; Laschewsky, A.; Tenhu, H. *Langmuir* **2002**, *18*, 5360−5365.
(24) Arotcarena, M.; Heise, B.; Ishaya, S.; Laschewsky, A. *J. Am. Chem. Soc.* **2002**, *124*, 3787−3793.

10.1021/la702029a CCC: $37.00
Published on Web 10/11/2007

Scheme 1

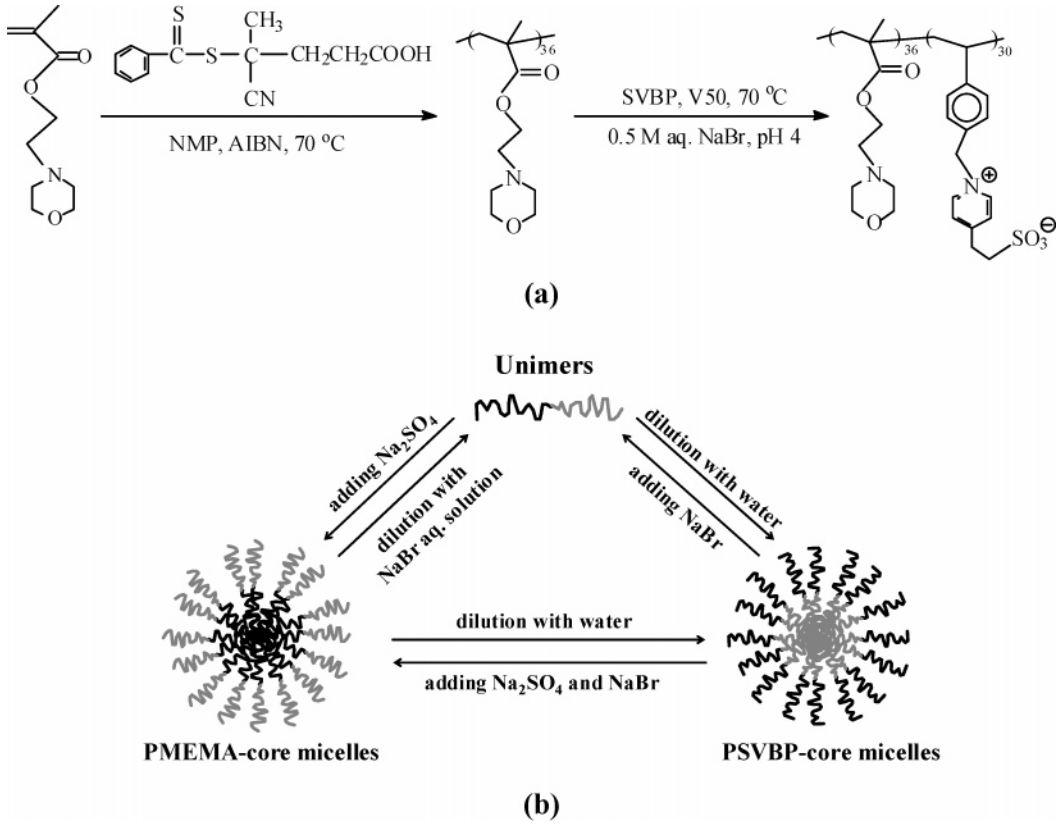

(a) Synthetic route of the synthesis of the PMEMA-*b*-PSVBP diblock copolymer. (b) Schematic illustration of the "schizophrenic" micellization behavior of the PMEMA-*b*-PSVBP diblock copolymer in aqueous solution at different conditions.

similar principles, Armes et al.[25] and Maeda et al.[26] reported more sophisticated examples.

It should be noted that practical applications of DHBC micelles might involve additives such as salts. The nature of salt and its concentration can exert a marked influence on the solution properties of water-soluble polymers and consequently the aggregation behavior of DHBCs.[27−30] To the best of our knowledge, DHBCs exhibiting purely salt-responsive "schizophrenic" micellization behavior have not been reported.

Poly(*N*-(morpholino)ethyl methacrylate) (PMEMA) is a weak polybase, and its conjugated acid possesses a pK_a of 4.9. It is molecularly soluble over a wide pH range, either as a weak cationic polyelectrolyte in acidic media or as a noncharged polymer at neutral or alkaline pH. Under the latter conditions, the water solubility of PMEMA is also salt-sensitive; that is, it can be salted out relatively easily from aqueous solution upon addition of divalent electrolytes such as Na_2SO_4 or K_2CO_3.[17,19] On the other hand, Laschewsky et al.[31] recently reported a new zwitterionic monomer, 4-(2-sulfoethyl)-1-(4-vinylbenzyl)pyridinium betaine (SVBP), and its polymer (PSVBP) was insoluble in most common organic solvents. Characteristic of polyzwitterions, PSVBP exhibits antipolyelectrolyte effects. It is insoluble in pure water but readily soluble in the presence of NaBr (>0.2 M). Thus, it is quite expected that poly(*N*-(morpholino)ethyl methacrylate)-*b*-poly(4-(2-sulfoethyl)-1-(4-vinylbenzyl)pyridinium betaine), PMEMA-*b*-PSVBP, might exhibit purely salt-responsive "schizophrenic" micellization behavior.

On the other hand, previous studies of DHBCs mainly focused on characterization of the equilibrium structures of micelles and "inverted" micelles. Like small molecule surfactants, the micellization kinetics of DHBCs is closely related to their stability, which plays an important role in various technological processes such as foaming, wetting, emulsification, solubilization, and detergency.[32,33] Our recent research interests involve the micellization processes, that is, micelle formation and inversion kinetics of "schizophrenic" DHBCs. Previously, we investigated the pH-induced micellization kinetics of an ABC triblock copolymer containing poly(2-(diethylamino)ethyl methacrylate) (PDEA) block.[34] We also reported the "schizophrenic" micellization behavior of a zwitterionic diblock copolymer, poly(4-vinylbenzoic acid)-*b*-poly(*N*-(morpholino)ethyl methacrylate) (PVBA-*b*-PMEMA),[19] and its micelle formation and inversion kinetics.[35] However, a general consensus concerning the micellization kinetics of DHBCs cannot be reached until more systems with different characteristics are explored.

Herein, we synthesized a novel double hydrophilic sulfobetaine block copolymer, PMEMA-*b*-PSVBP, which contains two salt-sensitive blocks, via reversible addition-fragmentation chain

(25) Weaver, J. V. M.; Armes, S. P.; Butun, V. *Chem. Commun.* **2002**, 2122−2123.
(26) Maeda, Y.; Mochiduki, H.; Ikeda, I. *Macromol. Rapid Commun.* **2004**, *25*, 1330−1334.
(27) He, E.; Ravi, P.; Tam, K. C. *Langmuir* **2007**, *23*, 2382−2388.
(28) Jain, N. J.; Aswal, V. K.; Goyal, P. S.; Bahadur, P. *J. Phys. Chem. B* **1998**, *102*, 8452−8458.
(29) Perreur, C.; Habas, J. P.; Lapp, A.; Peyrelasse, J. *Polymer* **2006**, *47*, 841−848.
(30) Ma, J. H.; Guo, C.; Tang, Y. L.; Wang, J.; Zheng, L.; Liang, X. F.; Chen, S.; Liu, H. Z. *Langmuir* **2007**, *23*, 3075−3083.
(31) Mertoglu, M.; Garnier, S.; Laschewsky, A.; Skrabania, K.; Storsberg, J. *Polymer* **2005**, *46*, 7726−7740.
(32) Noskov, B. A. *Adv. Colloid Interface Sci.* **2002**, *95*, 237−293.
(33) Patist, A.; Kanicky, J. R.; Shukla, P. K.; Shah, D. O. *J. Colloid Interface Sci.* **2002**, *245*, 1−15.
(34) Zhu, Z. Y.; Armes, S. P.; Liu, S. Y. *Macromolecules* **2005**, *38*, 9803−9812.
(35) Wang, D.; Yin, J.; Zhu, Z. Y.; Ge, Z. S.; Liu, H. W.; Armes, S. P.; Liu, S. Y. *Macromolecules* **2006**, *39*, 7378−7385.

transfer (RAFT) polymerization (Scheme 1a). In aqueous solution, PMEMA block becomes insoluble in the presence of Na_2SO_4 (>0.6 M), while PSVBP block molecularly dissolves in the presence of NaBr (>0.2 M). Thus, three different states, that is, unimer, PMEMA-core micelles, and PSVBP-core micelles, can be reached in aqueous solutions of PMEMA-*b*-PSVBP by adjusting the concentrations of salts (Scheme 1b). The equilibrium structures of PMEMA-core and PSVBP-core micelles were characterized by laser light scattering (LLS) and ^{1}H NMR. Moreover, the kinetics of salt-induced formation and dissociation of these two types of micelles and the structural inversion between them were explored by the stopped-flow light scattering technique.

Experimental Section

Materials. Methacryloyl chloride, *N*-(2-hydroxyethyl)morpholino, 2-(4-pyridine)ethanesulfonic acid, 2,2′-azobisisobutyronitrile (AIBN), and 4-vinylbenzyl chloride were purchased from Aldrich. 2,2′-Azobis(2-methylpropionamide) dihydrochloride (V50, Wako Pure Chemical Industries, LTD) was recrystallized from methanol. 4-Cyano-4-[(thiobenzoyl)sulfanyl]pentanoic acid was synthesized according to literature procedures.[36] *N*-Methyl-2-pyrrolidone (NMP), formamide, and all other chemicals were purchased from Shanghai Chemical Reagent Co. and used without further purification.

Sample Preparation. *Synthesis of 2-(N-Morpholino)ethyl Methacrylate (MEMA).* Methacryloyl chloride (24.4 mL, 1.2 equiv) in 20 mL of tetrahydrofuran (THF) was added dropwise into a THF solution (100 mL) of *N*-(2-hydroxyethyl)morpholino (25.0 mL, 1.0 equiv) and triethylamine (34.5 mL, 1.2 equiv) at 0 °C. The addition was complete within 2 h under the protection of dry N_2 atmosphere. The reaction was stirred for 12 h at room temperature. The reaction mixture was filtrated to remove the formed salt and then dried over anhydrous $MgSO_4$. After removing the solvents under reduced pressure, the residue was purified by vacuum distillation to give 13.0 g (31.6%) MEMA monomer as a colorless liquid (bp 78 °C /1.7 mbar). ^{1}H NMR ($CDCl_3$, ppm): δ = 1.88 (s, 3H), 4.25 (t, 2H), 2.62 (t, 2H), 2.48 (t, 4H), 5.5 (s, 2H), 6.0 (s, 2H).

Synthesis of 4-(2-Sulfoethyl)-1-(4-vinylbenzyl) Pyridinium Betaine (SVBP). 2-(4-Pyridine)ethanesulfonic acid (9.36 g, 0.05 mol) and NaOH (2.0 g, 0.05 mol) were dissolved in 60 mL of formamide. 4-Vinylbenzyl chloride (7.1 mL, 0.05 mol) containing a drop of 4-nitrobenzene was then added dropwise under N_2 atmosphere. The reaction mixture was stirred at room temperature for 60 h. After cooling to 5 °C, the mixture was precipitated into cold acetone, followed by filtration and drying in a vacuum oven overnight at room temperature. Crystallization from dry ethanol provided pure SVBP monomer. ^{1}H NMR and ^{13}C NMR results of the obtained monomer were consistent with those reported by Laschewsky et al.[31]

Preparation of PMEMA MacroRAFT Agent. RAFT polymerization was used to prepare the PMEMA macroRAFT agent and PMEMA-*b*-PSVBP diblock copolymer (Scheme 1a). In a typical example, MEMA (1.5 mL, 8 mmol), 4-cyano-4-[(thiobenzoyl)sulfanyl]-pentanoic acid (28 mg, 0.1 mmol), and AIBN (3 mg, 0.02 mmol) at a molar ratio of 400:5:1 were charged into a glass ampule containing 3 mL of NMP. The ampule was degassed via three freeze−pump−thaw cycles and flame-sealed under vacuum. It was then immersed into an oil bath preheated to 70 °C to start the polymerization. After 18 h, the ampule was quenched into liquid nitrogen to terminate the polymerization. The mixture was diluted with 3 mL of THF and then precipitated into an excess of *n*-hexane. This purification cycle was repeated twice. The obtained slightly pink powder was dried in a vacuum oven overnight at room temperature. The molecular weight and molecular weight distribution of PMEMA homopolymer were determined by aqueous gel permeation chromatography (GPC): M_n = 11 200, M_w/M_n = 1.25. The actual degree of polymerization (DP) of PMEMA homopolymer was determined to be 36 by ^{1}H NMR in $CDCl_3$. It was then employed as the maroRAFT agent for the preparation of the PMEMA-*b*-PSVBP diblock copolymer.

Preparation of PMEMA-b-PSVBP Diblock Copolymer. In a typical example, PMEMA macroRAFT agent (0.287 g, 0.04 mmol), SVBP (0.303 g, 1 mmol), and V50 (2 mg, 0.01 mmol) at a molar ratio of 5:125:1 were charged into a glass ampule containing 0.5 M NaBr aqueous solution (3 mL, pH ∼ 4). The mixture was degassed via three freeze−pump−thaw cycles and then flame-sealed under vacuum. The ampule was immersed into an oil bath thermostated at 80 °C to conduct the polymerization. After 12 h, the ampule was quenched into liquid nitrogen to stop the polymerization. Subsequently, the reaction mixture was dialyzed (MW cutoff = 7 000) against deionized water. A slightly pink powder (0.44 g, 76% yield) was obtained after freeze drying. The molecular weight and molecular weight distribution of PMEMA-*b*-PSVBP diblock copolymer were determined by aqueous GPC: M_n = 28 900, M_w/M_n = 1.18. The DP of PSVBP block was determined to be 30 by ^{1}H NMR in D_2O containing 0.5 M NaBr. The obtained diblock copolymer was denoted as $PMEMA_{36}$-*b*-$PSVBP_{30}$.

Characterization. *Nuclear Magnetic Resonance (NMR) Spectroscopy.* All ^{1}H and ^{13}C NMR spectra were recorded in D_2O or $CDCl_3$ using a Bruker 300 MHz spectrometer.

Gel Permeation Chromatography (GPC). The molecular weight and molecular weight distributions of the PMEMA homopolymer and PMEMA-*b*-PSVBP diblock copolymer were determined by aqueous GPC, using a Pharmacia Biotech "Superose 6" column (upper limit molecular weight was ∼ 4 × 10^7, flow rate was 0.50 mL/min, and column temperature was 20 °C) connected to a Polymer Labs ERC-7517A RI detector. The eluent was 0.40 M NaBr solution with a 50 μM Trizma buffer solution comprising equimolar amounts of tris(hydroxymethyl)aminomethane and tris(hydroxymethyl)-aminomethane hydrochloride (both purchased from Aldrich). Calibration was based on 14 poly(ethylene oxide) standards with the molar weights ranging from 440 to 288 000.

Laser Light Scattering (LLS). A commercial spectrometer (ALV/DLS/SLS-5022F) equipped with a multi-tau digital time correlator (ALV5000) and a cylindrical 22 mW UNIPHASE He−Ne laser (λ_0 = 632 nm) as the light source was employed for dynamic and static LLS measurements. In dynamic LLS, scattered light was collected at a fixed angle of 90° for a duration of 15 min. Distribution averages and particle size distributions were computed using cumulants analysis and CONTIN routines. All data were averaged over three separate measurements.

In static LLS, we can obtain the weight-average molar mass (M_w) and the *z*-average root-mean square radius of gyration ($\langle R_g^2 \rangle^{1/2}$ or written as $\langle R_g \rangle$) of polymer chains or aggregates in a dilute solution from the angular dependence of the excess absolute scattering intensity, known as the Rayleigh ratio $R_{vv}(q)$. The specific refractive index increments (d*n*/d*c*) were determined by a precise differential refractometer at 632 nm. It has been previously reported that the scattering contribution from small ions becomes significant only in very concentrated salt solutions, for example, in 3−4 M NaBr solutions.[37] Thus, this contribution is negligible in the current study. The molar mass of block copolymer micelles was measured at only one concentration (1 × 10^{-4} g/mL), and the extrapolation to zero concentration has not been conducted. Thus, the obtained molar mass should only be considered as an apparent value, denoted as $M_{w,app}$.

Transmission Electron Microscopy (TEM). TEM analyses were conducted on a Hitachi 800 transmission electron microscope at an acceleration voltage of 200 kV. Samples were prepared by placing 10 μL of micellar solution on copper grids coated with thin films of Formvar and carbon successively. No staining was required.

Stopped-Flow with Light-Scattering Detection.[38,39] Stopped-flow studies were carried out using a Bio-Logic SFM300/S stopped-flow instrument. It is equipped with three 10 mL step-motor-driven syringes (S1, S2, and S3), which can be operated independently to

(36) Thang, S. H.; Chong, Y. K.; Mayadunne, R. T. A.; Moad, G.; Rizzardo, E. *Tetrahedron Lett.* **1999**, *40*, 2435−2438.

(37) Sedlak, M. *Surfactant Science Series*; Redeva, T., Ed.; Marcel Dekker Inc.: New York, 2001.

(38) Bednar, B.; Edwards, K.; Almgren, M.; Tormod, S.; Tuzar, Z. *Makromol. Chem., Rapid Commun.* **1988**, *9*, 785−790.

(39) Johnson, K. A. *Kinetic Analysis of Macromolecules: A Practical Approach*; Oxford University Press: New York, 2003.

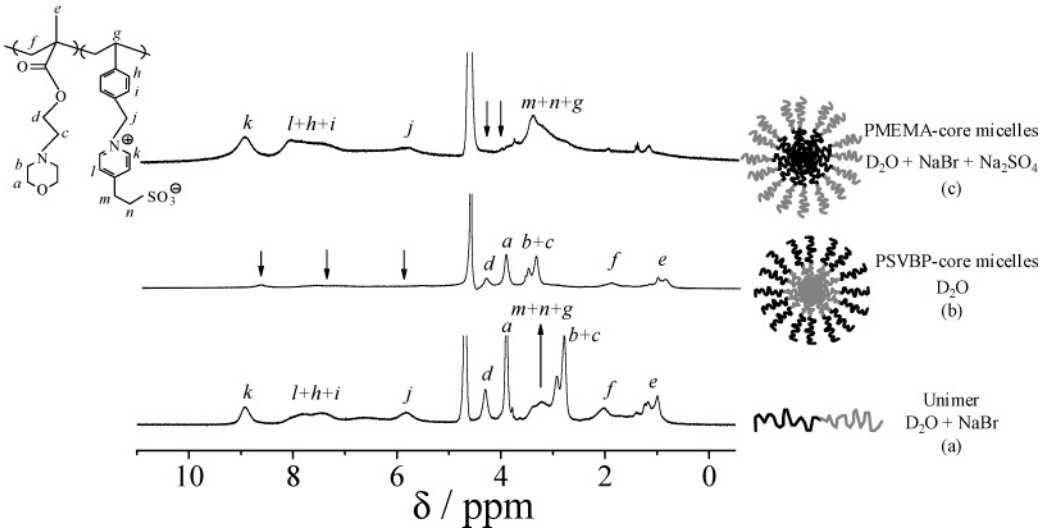

Figure 1. ^{1}H NMR spectra recorded for PMEMA-*b*-PSVBP: (a) in D_2O with 0.5 M NaBr (pH 7); (b) in D_2O (pH 3); and (c) in D_2O with 0.8 M Na_2SO_4 and 0.5 M NaBr.

carry out single- or double-mixing. The stopped-flow device is attached to a MOS-250 spectrometer; kinetic data were fitted using the Biokine program provided by Bio-Logic. For light scattering detection at a scattering angle of 90°, both the excitation and emission wavelengths were adjusted to 335 nm with 10 nm slits. Using FC-08 or FC-15 flow cells, typical dead times are 1.1 and 2.6 ms, respectively. The solution temperature was maintained at 25 °C by circulating water around the syringe chamber and the observation head. All solutions prior to loading into the motor-driven syringes were clarified by 0.45 μm Millipore Nylon filters.

Results and Discussion

Synthesis of PMEMA-*b*-PSVBP. The target block copolymer was synthesized by consecutive RAFT polymerizations of MEMA and SVBP monomers (Scheme 1a). First, MEMA was polymerized at 70 °C using 4-cyano-4-[(thiobenzoyl)sulfanyl]pentanoic acid as the RAFT agent. The ^{1}H NMR spectrum of PMEMA in $CDCl_3$ revealed the presence of characteristic signals at $\delta = 3.9$ and 4.4 ppm. Signals at $\delta = 7.9$, 7.6, and 7.4 ppm were ascribed to protons of the dithiobenzoyl terminal group at the PMEMA chain end. Aqueous GPC analysis gave a monomodal peak with $M_n \sim 11\,200$ and a polydispersity, M_w/M_n, of 1.25. The actual degree of polymerization, DP, of PMEMA was determined to be 36 by ^{1}H NMR.

Laschewsky et al. originally reported the preparation of SVBP monomer and its RAFT polymerization.[31] SVBP was typically polymerized as a second monomer using an appropriate macroRAFT agent, affording the target diblock copolymers. In the current case, the above obtained PMEMA was employed as the macroRAFT agent for the polymerization of SVBP, leading to the formation of the PMEMA-*b*-PSVBP diblock copolymer. The ^{1}H NMR spectrum of the obtained diblock copolymer in D_2O (0.5 M NaBr) revealed the presence of characteristic signals of both blocks (Figure 1a). Aqueous GPC analysis showed that the elution peak of PMEMA-*b*-PSVBP shifts to a higher molecular weight, compared to that of the PMEMA precursor. Most importantly, the elution peak of the diblock copolymer was relatively symmetric and exhibited no tailing at the lower molecular weight side, indicating the complete consumption of the PMEMA macroRAFT agent.

"Schizophrenic" Micellization Behavior of PMEMA-*b*-PSVBP. At neutral or alkaline pH, PMEMA homopolymer dissolves molecularly at room temperature and becomes insoluble in the presence of >0.6 M Na_2SO_4. It should be noted that the salt-sensitive water solubility of PMEMA is quite selective to the type of salt. Preliminary experiments revealed that, even in the presence of 2.0 M NaBr, PMEMA homopolymer can molecularly dissolve in water at 25 °C. As reported by Laschewsky et al.,[31] PSVBP homopolymer exhibits antipolyelectrolyte behavior. It is insoluble in pure water but readily soluble in the presence of >0.2 M NaBr. However, like other polybetaines possessing different water solubilities in the presence of different types of salt,[40−42] divalent salts such as Na_2SO_4 (<1.0 M) exhibit no such effects on the promotion of the water solubility of PSVBP homopolymers. As the two blocks exhibit different salt-sensitive water solubilities, we expect that PMEMA-*b*-PSVBP might exhibit the "schizophrenic" micellization behavior upon dually playing with the concentrations and/or types of salt, that is, NaBr and Na_2SO_4 (Scheme 1b).

Figure 1 shows the ^{1}H NMR spectra recorded for PMEMA-*b*-PSVBP in D_2O at different conditions. Both blocks are fully solvated in D_2O containing 0.5 M NaBr, and characteristic signals of both PMEMA and PSVBP blocks are visible (Figure 1a, note the prominent signals at 3.9 and 4.4 ppm characteristic of PMEMA block and that at 5.6−5.8 and 7.0−9.0 ppm characteristic of PSVBP block). PSVBP block is insoluble in the absence of any salts, and colloidal aggregates apparently form as indicated by the bluish tinge characteristic of micellar aggregates. ^{1}H NMR resonance signals characteristic of PSVBP block ($\delta = 5.6-5.8$, 7.0−8.0, and 9.0 ppm) are suppressed to a large extent, while the characteristic PMEMA signal at $\delta = 3.9$ and 4.4 ppm is clearly visible (Figure 1b). This indicates the formation of PSVBP-core micelles, stabilized by the well-solvated PMEMA corona. On the other hand, PMEMA block is water-insoluble and PSVBP is soluble in the presence of 0.5 M NaBr and 0.8 M Na_2SO_4. The ^{1}H NMR spectrum reveals the complete disappearance of characteristic PMEMA signals at $\delta = 3.9$ and 4.4 ppm, suggesting the formation of PMEMA-core micelles (Figure 1c). This conclusion was further corroborated by the fact that characteristic PSVBP signals at $\delta = 5.6-5.8$, 7.0−8.0, and 9.0 ppm are clearly evident. This strongly suggests the formation of PSVBP-core micelles stabilized with well-solvated PMEMA coronas. A schematic illustration of the "schizophrenic" micellization behavior of PMEMA-*b*-PSVBP is shown in Scheme 1b.

(40) Lowe, A. B.; McCormick, C. L. *Chem. Rev.* **2002**, *102*, 4177−4189.
(41) Soto, V. M. M.; Galin, J. C. *Polymer* **1984**, *25*, 121−128.
(42) Salamone, J. C.; Volksen, W.; Olson, A. P.; Israel, S. C. *Polymer* **1978**, *19*, 1157−1162.

Table 1. Dynamic and Static LLS Characterization of PMEMA-Core Micelles and "Inverted" PSVBP-Core Micelles Formed by the $PMEMA_{36}$-*b*-$PSVBP_{30}$ Diblock Copolymer in Aqueous Solution at Different Conditions

micelle parameters	$PMEMA_{36}$-*b*-$PSVBP_{30}$ unimer (0.5 M NaBr)	PSVBP-core micelles (no salt)	PMEMA-core micelles (0.5 M NaBr and 0.8 M Na_2SO_4)
$M_{w,app}$	5.4×10^4	2.3×10^6	1.5×10^7
$\langle R_g \rangle$ (nm)		15	29
$\langle R_h \rangle$ (nm)	5	22	38
$\langle R_g \rangle / \langle R_h \rangle$		0.68	0.76
N_{agg}	1−2	43	278
$\langle \rho \rangle$ (g/cm^3)		0.09	0.11
d*n*/d*c* (mL/g)	0.138	0.131	0.185

Thus, three different states, that is, unimer, PMEMA-core micelles, and PSVBP-core micelles, can be independently reached in the aqueous solution of PMEMA-*b*-PSVBP by selectively tuning the water solubility of each block with NaBr and/or Na_2SO_4 concentrations. Static and dynamic LLS were then employed to characterize the equilibrium structures of these two types of micelles with "inverted" nanostructures. Table 1 summarizes the structural parameters of unimers, PSVBP-core micelles, and PMEMA-core micelles formed at different conditions in aqueous solution. PMEMA-core micelles formed in the presence 0.5 M NaBr and 0.8 M Na_2SO_4 were much larger than PSVBP-core micelles formed in the absence of any salts. As both blocks possess comparable chain lengths, the difference in the micelle size should be due to the presence of salt in the former case, which can render the insoluble PMEMA block more hydrophobic. This shift in the overall hydrophilic-hydrophobic balance will inevitably lead to larger micellar aggregates. Further LLS studies revealed that the micelle formation and dissociation and the structural inversion of these two types of micelles were fully reversible if the concentrations and types of added salts were carefully tuned.

Static LLS studies of the PMEMA-core and PSVBP-core micelles yielded apparent weight-average molar masses, $M_{w,app}$, of approximately 1.5×10^7 and 2.3×10^6 g/mol, respectively (see Table 1). Based on the weight-average molar mass of the $PMEMA_{36}$-*b*-$PSVBP_{30}$ diblock copolymer determined by static LLS in the presence of 0.5 M NaBr (i.e., under these conditions, the diblock copolymer is assumed to be molecularly dissolved), the micelle aggregation numbers (N_{agg}) were estimated to be 278 and 43 for PMEMA-core and PSVBP-core micelles, respectively. Using the equation $\langle \rho \rangle = M_w/(4/3\pi N_a \langle R_h \rangle^3)$, the average micelle densities, $\langle \rho \rangle$, of PMEMA-core and PSVBP-core micelles were estimated to be 0.11 and 0.09 g/cm, respectively. The $\langle R_g \rangle / \langle R_h \rangle$ ratios for PMEMA-core and PSVBP-core micelles were calculated to be 0.76 and 0.68, respectively, which were close to the theoretical value of 0.774 predicted for nondraining hard spheres.

This morphology of PSVBP-core micelles was further confirmed by TEM observation (see the Supporting Information, Figure S1), revealing the presence of spherical nanoparticles of ~20 nm. Due to the presence of a high concentration of salts (0.8 M Na_2SO_4 and 0.5 M NaBr), direct TEM observation of PMEMA-core micelles was not possible. However, dynamic LLS studies at different angles revealed that the $\langle R_h \rangle$ values of PMEMA-core micelles were almost independent of the scattering vectors. The weak angular dependence of $\langle R_h \rangle$ strongly suggested that PMEMA-core micelles should take spherical shapes.

Kinetics of Micelle Formation and Inversion. It should be noted that the above LLS measurements were conducted ~4 h after adjusting the salt concentrations. We assume that, after this period of storage, the micelles are close to their equilibrium state. Semenov et al.[43,44] proposed theoretically that the unimer-to-micelle transition can only be characterized by a continuous spectrum of relaxation times, ascribing to increasing energy barriers with growing N_{agg}. Moreover, they emphasized that the growing micelles may never reach the final equilibrium state and their growth can be arrested at an intermediate stage. For kinetic studies in the current case, we only focused on the early stages of the micelle formation and inversion processes, during which the most dramatic changes should occur. At later stages of the unimer-to-micelle transition or structural inversion, we believe that the relaxation into the final equilibrium state should actually follow equilibrium exchange kinetics, the study of which has been relatively mature.[45−48]

For the early stage kinetics of micelle formation and inversion, the stopped-flow apparatus provides a suitable technique with a time resolution down to a few milliseconds.[34,38] The time dependence of the scattered light intensity at 90° was recorded following the abrupt jump of salt concentrations by stopped-flow mixing.

Kinetics of Salt-Induced Formation and Dilution-Induced Breakup of PMEMA-Core Micelles. Figure 2 shows the time dependence of the scattered light intensity obtained after stopped-flow mixing of the aqueous solution of PMEMA-*b*-PSVBP with the aqueous Na_2SO_4 solution at 25 °C; the final copolymer concentration was fixed at 0.6 g/L, and the final Na_2SO_4 concentration was varied. If the final Na_2SO_4 concentration is less than 0.5 M, the kinetic trace remains flat, suggesting that the diblock copolymer chains molecularly dissolve, that is, no micelles form. In the final Na_2SO_4 concentraion range of 0.52−0.6 M, the scattered light intensity increases gradually. On the other hand, the scattered intensity increases abruptly and then stabilizes out within ~2−3 s at a final Na_2SO_4 concentration of >0.6 M. The abrupt increase of the scattered intensity suggests the salt-induced formation of PMEMA-core micelles (Scheme 1b).

Apparently, we can also observe from Figure 2b that the micelles form faster at increasing Na_2SO_4 concentrations. The time dependence of the scattered light intensity (I_t) can be normalized using $(I_\infty - I_t)/I_\infty$ versus t, where I_∞ is the value of I_t at an infinitely long time. The dynamic traces obtained in the presence of 0.52−0.6 M Na_2SO_4 can be fitted with single-exponential functions. In the presence of >0.64 M Na_2SO_4, kinetic traces can only be well-fitted with double-exponential functions:

$$\frac{I_\infty - I_t}{I_\infty} = c_1 e^{-t/\tau_1} + c_2 e^{-t/\tau_2} \quad (1)$$

where c_1 and c_2 are the normalized amplitudes ($c_2 = 1 - c_1$) and τ_1 and τ_2 are the characteristic relaxation times for two processes such that $\tau_1 < \tau_2$. The characteristic relaxation time for the overall micelle formation process, τ_f, can be calculated as

$$\tau_f = c_1\tau_1 + c_2\tau_2 \quad (2)$$

Figure 3 shows the double-exponential fitting results of the dynamic traces shown in Figure 2. Both τ_1 and τ_2 decrease with increasing Na_2SO_4 concentrations. The calculated τ_f for the overall

(43) Nyrkova, I. A.; Semenov, A. N. *Macromol. Theory Simul.* **2005**, *14*, 569−585.
(44) Nyrkova, I. A.; Semenov, A. N. *Faraday Discuss.* **2005**, *128*, 113−127.
(45) Haliloglu, T.; Bahar, I.; Erman, B.; Mattice, W. L. *Macromolecules* **1996**, *29*, 4764−4771.
(46) Smith, C. K.; Liu, G. J. *Macromolecules* **1996**, *29*, 2060−2067.
(47) Wang, Y. M.; Kausch, C. M.; Chun, M. S.; Quirk, R. P.; Mattice, W. L. *Macromolecules* **1995**, *28*, 904−911.
(48) Underhill, R. S.; Ding, J. F.; Birss, V. I.; Liu, G. J. *Macromolecules* **1997**, *30*, 8298−8303.

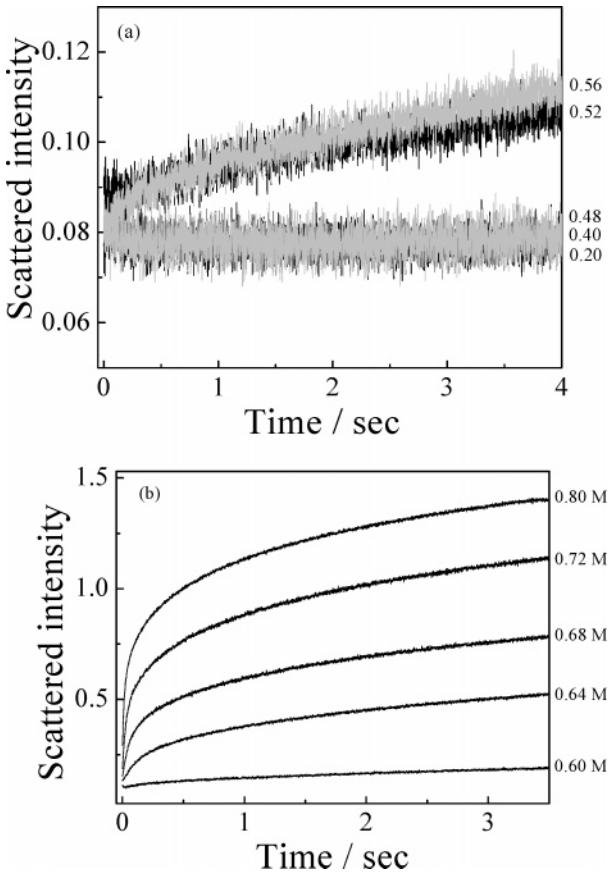

Figure 2. Time dependence of the scattered light intensity obtained after stopped-flow mixing an aqueous solution of PMEMA-*b*-PSVBP copolymer (at 2.0 g/L) with an aqueous Na_2SO_4 solution at 25 °C. From bottom to top, the final Na_2SO_4 concentrations were (a) 0.20, 0.40, 0.48, 0.52, and 0.56 M and (b) 0.60, 0.64, 0.68, 0.72, and 0.80 M. The final copolymer concentration was fixed at 0.6 g/L. All solutions prior to mixing contained 0.5 M NaBr.

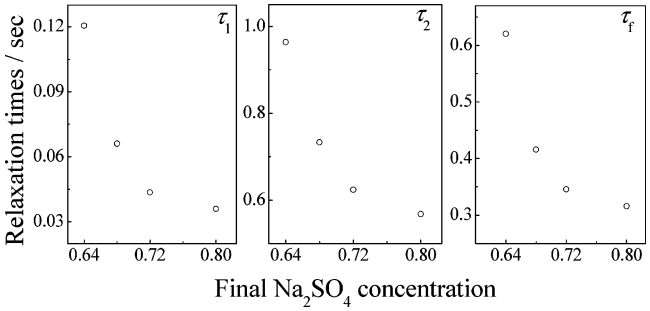

Figure 3. Double-exponential fitting results of kinetic traces obtained for the formation of PMEMA-core micelles at varying final Na_2SO_4 concentrations. The experimental conditions were the same as those described in Figure 2.

micellization process is in the range of 0.3−0.6 s, and it also decreases with increasing Na_2SO_4 concentrations. The driving force for the formation of PMEMA-core micelles is the addition of Na_2SO_4, which renders the PMEMA block insoluble. Thus, it is quite reasonable to expect that at increasing Na_2SO_4 concentrations, the driving force for micellization becomes larger and consequently the micellization kinetics becomes faster.

Figure 4 shows the time dependence of the scattered light intensity upon mixing the aqueous solution of PMEMA-*b*-PSVBP at different concentrations with aqueous Na_2SO_4 solution under stopped-flow conditions. All solutions prior to mixing contain 0.5 M NaBr, and the final Na_2SO_4 concentration was fixed at 0.8 M. When the final copolymer concentration was ≥0.2 g/L,

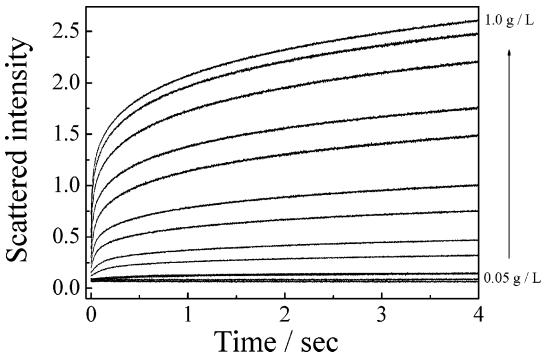

Figure 4. Time dependence of the scattered light intensity obtained after stopped-flow mixing an aqueous solution of PMEMA-*b*-PSVBP copolymer with an aqueous Na_2SO_4 solution at 25 °C. From bottom to top, the final copolymer concentrations were 0.05, 0.1, 0.15, 0.2, 0.25, 0.3, 0.4, 0.5, 0.6, 0.7, 0.8, 0.9, and 1.0 g/L. The final Na_2SO_4 concentration was fixed at 0.8 M. All solutions prior to mixing contained 0.5 M NaBr.

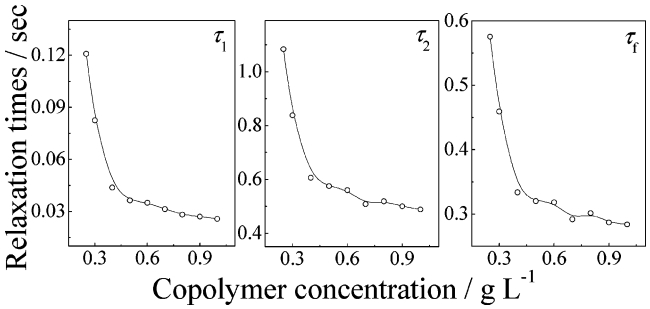

Figure 5. Double-exponential fitting results of kinetic traces obtained for the formation of PMEMA-core micelles at various final copolymer concentrations. The experimental conditions were the same as those described in Figure 4.

an increase of the scattered intensity could be clearly observed, suggesting the formation of PMEMA-core micelles above the critical micelle concentration (cmc). Figure 5 shows the double-exponential fitting results, revealing that both τ_1 and τ_2 decrease with increasing copolymer concentrations.

Following similar principles in interpreting the previously reported pH- and salt-induced micellization kinetics,[34,35] the salt-induced formation of PMEMA-core micelles should follow two consecutive processes. In the fast process (τ_1), unimers quickly associate into small micelles; the fusion between these nascent micelles results in the formation of quasi-equilibrium micelles. The slow process (τ_2) is associated with micelle formation/breakup, approaching the final equilibrium state. The decrease of τ_2 with increasing copolymer concentrations strongly suggests that the slow process proceeds via the micelle fusion/fission mechanism, probably due to the presence of a high concentration of salts (0.8 M Na_2SO_4).

The dissociation of PMEMA-core micelles into unimers can be induced by dilution with aqueous NaBr solution, which can decrease the Na_2SO_4 concentration and keep the NaBr concentration constant at 0.5 M. Under these conditions, PSVBP block remains soluble and PMEMA block becomes soluble due to decreased Na_2SO_4 concentration, leading to the micelle-to-unimer transition of PMEMA-core micelles (Scheme 1b). The stopped-flow technique can conveniently monitor this process, and the results are shown in Figure 6.

Depending on the final Na_2SO_4 concentration, the relaxation curves can be categorized into four types. In the final Na_2SO_4 concentration range of 0.6−0.8 M, the scattered intensity only exhibits moderate changes, indicating that PMEMA-core micelles

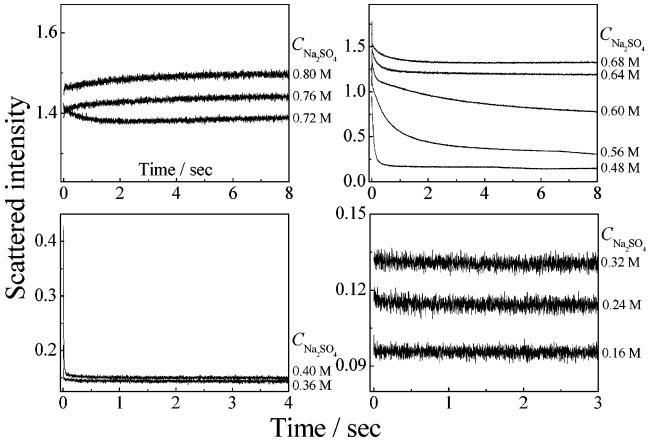

Figure 6. Time dependence of the scattered light intensity obtained after diluting an aqueous solution of PMEMA-*b*-PSVBP (5.0 g/L, 0.8 M Na_2SO_4, and 0.5 M NaBr) with different volumes of aqueous NaBr solution (0.5 M). The final copolymer concentration was fixed at 1.0 g/L.

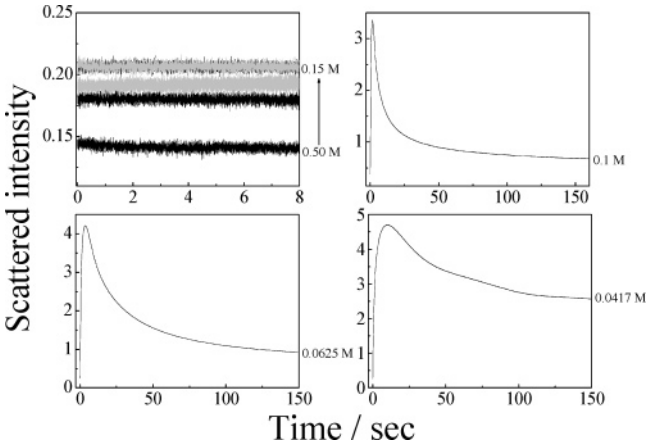

Figure 7. Time dependence of the scattered light intensity obtained after diluting an aqueous solution of PMEMA-*b*-PSVBP (5.0 g/L, 0.16 M Na_2SO_4, and 0.5 M NaBr) with different volumes of aqueous Na_2SO_4 solution (0.16 M). The final NaBr concentrations after mixing are denoted.

are still present, although partial structural rearrangement may occur. In the final Na_2SO_4 concentration range of 0.4−0.6 M, a more prominent decrease of the scattered intensity can be observed, suggesting partial micelle disintegration and a decrease of N_{agg}. At a final Na_2SO_4 concentration of ≤0.4 M, the scattered intensity abruptly decreases within ∼40 ms, indicating a complete micelle-to-unimer transition. Finally, below ∼0.3 M Na_2SO_4, the dissociation of PMEMA-core micelles into unimers occurs completely within the dead time of the stopped-flow apparatus (∼2−3 ms). The dissociation kinetics of PMEMA-core micelles is in general agreement with its formation process (Figure 2). The lower the final Na_2SO_4 concentration, the larger the driving force for the micelle-to-unimer transition, and the faster the micelle disintegration kinetics.

Kinetics of Dilution-Induced Formation and Salt-Induced Breakup of PSVBP-Core Micelles. Figure 7 shows the time dependence of the scattered intensity obtained after diluting an aqueous solution of PMEMA-*b*-PSVBP (5.0 g/L, 0.16 M Na_2SO_4, and 0.5 M NaBr) with different volumes of aqueous Na_2SO_4 solution (0.16 M). If the final NaBr concentration is >0.1 M, the kinetics trace remains a straight line, suggesting that the copolymer chains remain molecularly soluble and no micelles form. At a final NaBr concentration of ≤0.1 M, the scattered intensity abruptly increases to a maximum and then gradually decreases to stabilize out; the final scattered intensity value is larger than that of the unimer state. This suggests the dilution-induced formation of PSVBP-core micelles (Scheme 1b).

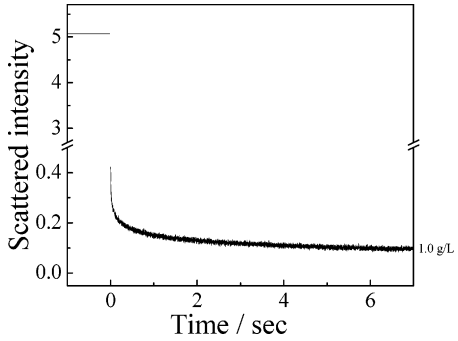

Figure 8. Time dependence of the scattered light intensity obtained after diluting an aqueous solution of PMEMA-*b*-PSVBP copolymer (2.0 g/L) with an equal volume of aqueous NaBr solution (1.0 M). The final copolymer and NaBr concentrations were 1.0 g/L and 0.5 M, respectively.

The appearance of a maximum indicates that the formation of PSVBP-core micelles follows different kinetic sequences compared to that of PMEMA-core micelles. Upon abruptly decreasing NaBr concentrations, PMEMA-*b*-PSVBP unimers quickly associate into large aggregates due to the insolubility of the zwitterionic PSVBP block; the aggregates then rearrange and gradually relax into smaller and more stable PSVBP-core micelles. We can also tell from Figure 7 that the lower the final NaBr concentration, the slower the initial increase of scattered intensity, and the larger the final equilibrium scattered light intensity.

The dissociation of PSVBP-core micelles into unimers can be conveniently induced by increasing NaBr concentrations (Scheme 1b). Figure 8 shows a typical dynamic trace obtained for the micelle-to-unimer transition of PSVBP-core micelles. Single-exponential fitting leads to a characteristic relaxation time (τ_d) of ∼0.3 s. It should be noted that τ_d does not change with final copolymer concentrations. Compared to the dilution-induced dissociation kinetics of PMEMA-core micelles at a final Na_2SO_4 concentration <0.3 M (Figure 6), the salt-induced dissociation of PSVBP-core micelles is much slower. This difference leads to intriguing kinetics of structural inversion between these two types of micelles.

Kinetics of Structural Inversion from PSVBP-Core to PMEMA-Core Micelles. PMEMA-*b*-PSVBP forms PSVBP-core micelles in the absence of any salts. Upon simultaneous addition of Na_2SO_4 (0.8 M) and NaBr (0.5 M), PSVBP-core micelles can transform into structurally inverted PMEMA-core micelles (Scheme 1b). Figure 9 shows the time dependence of the scattered light intensity during the structural inversion from PSVBP-core to PMEMA-core micelles at different final copolymer concentrations.

If the final copolymer concentration is ≤0.15 g/L, no relaxation process can be observed, suggesting that the concentration is below the cmc of the PMEMA-core micelles. This is also in agreement with the formation kinetics of PMEMA-core micelles (Figure 4). In the final polymer concentrations range of 0.4−0.6 g/L, the scattered intensity gradually increases and then stabilizes out.

Interestingly, at even higher copolymer concentrations (≥0.7 g/L), the scattered intensity abruptly increases to a maximum and then slowly decreases. We have established in the previous section that the characteristic relaxation time (τ_d) for the micelle-

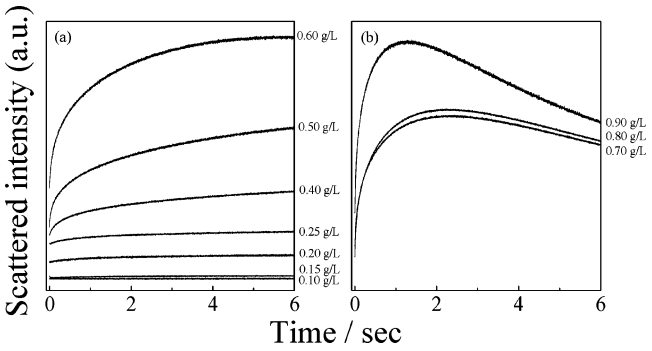

Figure 9. Time dependence of the scattered light intensity obtained after stopped-flow mixing an aqueous solution of PMEMA-*b*-PSVBP with aqueous Na_2SO_4 and NaBr solutions at 25 °C. From bottom to top, the final copolymer concentrations were (a) 0.10, 0.15, 0.20, 0.25, 0.40, 0.50, and 0.60 g/L and (b) 0.70, 0.80, and 0.90 g/L. The final Na_2SO_4 and NaBr concentrations were fixed at 0.8 and 0.5 M, respectively.

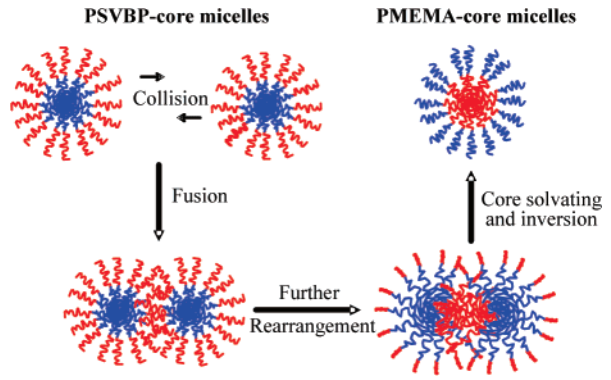

Figure 10. Schematic illustration of the possible kinetic sequences involved in the structural inversion from PSVBP-core to PMEMA-core micelles at relatively high block copolymer concentrations (≥0.7 g/L).

to-unimer transition of PSVBP-core micelles is ~0.3 s, and it remains almost constant with polymer concentrations (Figure 8).

The appearance of a scattered intensity maximum at relatively high polymer concentrations can be rationalized as follows. At higher concentrations, the diffusion-limited fusion between unstable PSVBP-core micelles possessing insoluble PMEMA coronas will be more prominent, whereas the rate of the dissociation of PSVBP-core micelles into unimers remains relatively unchanged. The subsequent decrease of scattered intensity can be ascribed to the disintegration of fused aggregates, accompanied with the solvation of PSVBP-core blocks and the formation of PMEMA cores.

A schematic illustration of the possible kinetic sequences involved in the structural inversion from PSVBP-core into PMEMA-core micelles at a final polymer concentration of ≥0.7 g/L is shown in Figure 10. Immediately after the salt jump, PMEMA corona chains become insoluble, and PSVBP-core micelles partially disintegrate into unimers at the same time. The remaining colloidally unstable PSVBP-core micelles undergo intermicellar fusion; the PSVBP cores of the fused aggregates then become solvated, and finally colloidally stable PMEMA-core micelles form.

Kinetics of Structural Inversion from PMEMA-Core to PSVBP-Core Micelles. In the presence of 0.8 M Na_2SO_4 and 0.5 M NaBr, PMEMA-core micelles form. Simple dilution with water leads to a concomitant decrease of the concentration of both

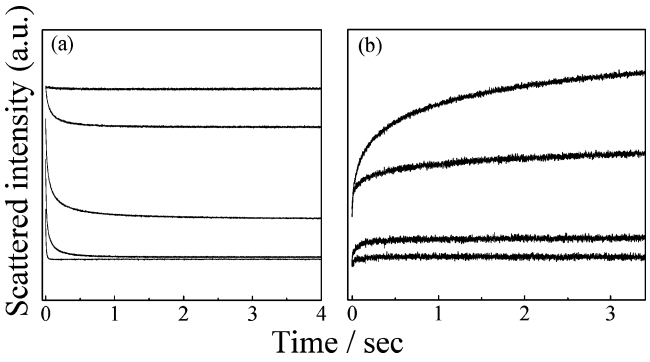

Figure 11. Time dependence of the scattered light intensity obtained after stopped-flow mixing an aqueous solution of PMEMA-*b*-PSVBP (5.0 g/L, 0.8 M Na_2SO_4, and 0.5 M NaBr) with different volumes of water at 25 °C. (a) From top to bottom, the final Na_2SO_4 and NaBr concentrations were 0.8/0.5, 0.72/0.45, 0.64/0.4, 0.56/0.35, and 0.48/0.3 M, respectively. (b) From bottom to top, the final Na_2SO_4 and NaBr concentrations were 0.4/0.25, 0.32/0.2, 0.24/0.15, and 0.16/0.1 M, respectively. The final copolymer concentration was fixed at 1.0 g/L.

salts. As the critical Na_2SO_4 and NaBr concentrations to induce the insolubility of PMEMA block and the solubility of PSVBP block in aqueous solution are 0.6 and 0.2 M, respectively, initial dilution leads to the breakup of PMEMA-core micelles into unimers, and further dilution results in the formation of structurally "inverted" PSVBP-core micelles (Scheme 1b).

Subjected to an abrupt stopped-flow dilution, Figure 11a shows typical kinetics of the dissociation of PMEMA-core micelles. From Figure 11b, we can tell that the scattered light intensity monotonically increases with time and then stabilizes out when the final NaBr concentrations are less than 0.15 M. This indicates the structural inversion from PMEMA-core to PSVBP-core micelles. As discussed in previous sections, the micelle-to-unimer transition of PMEMA-core micelles completes within the stopped-flow dead time when the final Na_2SO_4 concentration is <0.3 M (Figure 6). As no maximum in the scattered intensity is observed in Figure 11b, the inversion from PMEMA-core to PSVBP-core micelles should proceed first with the fast breakup of PMEMA-core micelles into unimers, followed by the remicellization into PSVBP-core micelles.

Conclusion

In summary, we reported the first example of purely salt-responsive "schizophrenic" micellization behavior based on a novel double hydrophilic sulfobetaine diblock copolymer, poly(*N*-(morpholino)ethyl methacrylate)-*b*-poly(4-(2-sulfoethyl)-1-(4- vinylbenzyl)pyridinium betaine) (PMEMA-*b*-PSVBP). Depending on the type and concentration of the salts (Na_2SO_4 and NaBr), two types of micelles, that is, PMEMA-core and PSVBP-core micelles, can form in aqueous solution. The kinetics of formation, breakup, and structural inversion of these two types of micelles were studied by the stopped-flow light scattering technique, and possible mechanisms were explored. The dilution-induced dissociation of PMEMA-core micelles into unimers occurs within the dead time of the stopped-flow apparatus (~2−3 ms) if the final Na_2SO_4 concentration is <0.3 M, while the salt-induced breakup of PSVBP-core micelles is considerably slower. Moreover, the kinetic sequences associated with the structural inversion between PMEMA-core and PSVBP-core micelles are mainly determined by the dissociation rate of the initial micelles and the intermicellar fusion rate after the micellar corona is

rendered water-insoluble. The latter mainly depends on the proximity of the neighboring micelles, that is, block copolymer concentrations.

Acknowledgment. This work was financially supported by an Outstanding Youth Fund (50425310) and research grants (20534020 and 20674079) from the National Natural Scientific Foundation of China (NNSFC), the "Bai Ren" Project and Special Grant (KJCX2-SW-H14) of the Chinese Academy of Sciences, and the Program for Changjiang Scholars and Innovative Research Team in University (PCSIRT).

Supporting Information Available: TEM image of PSVBP-core micelles formed in aqueous solution. This material is available free of charge via the Internet at http://pubs.acs.org.

LA702029A